Caryologia
International Journal of Cytology, Cytosystematics and Cytogenetics

Firenze University Press
www.fupress.com/caryologia

OPEN ACCESS

Citation: Luțu, O.A., Soare, L.C., Fierăscu, I., Fierăscu, R.-C., Dobrescu, C.M., Păunescu, A., Ponepal, C.M., Topală, C.M., Vîjan, L.E., Deliu, I., Negrea, D., Vîlcoci, D.Ș., Cîrstea, G., Aldea, F., Honțaru, S.O., & Șuțan, N.A. (2024). Phytotoxicity, cytogenotoxicity and antimicrobial potential of extracts with gold-silver bimetallic nanoparticles obtained from pteridophyte spores. *Caryologia* 77(1): 65-82. doi: 10.36253/caryologia-2424

Received: December 13, 2023

Accepted: May 21, 2024

Published: July 8, 2024

Data Availability Statement: All relevant data are within the paper and its Supporting Information files.

Competing Interests: The Author(s) declare(s) no conflict of interest.

ORCID
OAL: 0000-0001-8351-0919
LCS: 0000-0002-2874-3135
IF: 0000-0002-1834-9812
RCF: 0000-0003-4224-9157
CMD: 0000-0001-7972-3612
AP: 0000-0002-0228-4524
CMP: 0000-0002-0391-7629
CMT: 0000-0002-9117-4983
LEV: 0000-0003-1607-4947
DN: 0000-0001-7525-1056
DSV: 0000-0002-9777-6782
GC: 0000-0002-7442-7109
NAS: 0000-0001-7459-628X

Phytotoxicity, cytogenotoxicity and antimicrobial potential of extracts with gold-silver bimetallic nanoparticles obtained from pteridophyte spores

Oana Alexandra Luțu[1], Liliana Cristina Soare[1,*], Irina Fierăscu[2,3], Radu-Claudiu Fierăscu[2,4], Codruța Mihaela Dobrescu[1], Alina Păunescu[1], Cristina Maria Ponepal[1], Carmen Mihaela Topală[1], Loredana Elena Vîjan[1], Ionica Deliu[1], Denis Negrea[5], Denisa Ștefania Vîlcoci[5], Georgiana Cîrstea[5], Florentina Aldea[6], Sorina Octavia Honțaru[7], Nicoleta Anca Șuțan[1]

[1] *Department of Natural Sciences, Faculty of Science, Physical Education and Informatics, National University of Science and Technology Politehnica Bucharest, Pitesti University Center, Romania, 1 Targu din Vale Str., 110040 Pitesti, Romania*
[2] *The National Institute for Research & Development in Chemistry and Petrochemistry, ICECHIM, 202 Spl. Independentei, 060021 Bucharest, Romania*
[3] *Faculty of Horticulture, University of Agronomic Sciences and Veterinary Medicine of Bucharest, 59 Marasti Bvd., 011464 Bucharest, Romania*
[4] *Faculty of Chemical Engineering and Biotechnology, National University of Science and Technology Politehnica Bucharest, 1-7 Gheorghe Polizu St., 011061 Bucharest, Romania*
[5] *Regional Research and Development Center for Innovative Materials, Processes and Products for the Automotive Industry (CRC&D-Auto), National University of Science and Technology Politehnica Bucharest, Pitesti University Center, Romania, 1 Targu din Vale Str., 110040 Pitesti, Romania*
[6] *Department of Developmental Biology, Institute of Biology-Bucharest, Romanian Academy, 296 Splaiul Independentei Street, 060031 Bucharest, Romania*
[7] *Department of Health Care and Physiotherapy, Faculty of Sciences, Physical Education and Informatics, National University of Science and Technology Politehnica Bucharest, Pitesti University Center, Romania, 1 Targu din Vale Str., 110040 Pitesti, Romania*
*Corresponding author. Email: liliana.soare@upb.ro

Abstract. Investigating the toxicity of naturally occurring or synthesized nanoparticles for various applications is absolutely necessary for environmental protection and safety use. The aim of these research was to investigated the phytotoxicity, cytogenotoxicity and antibacterial potential of the extracts with gold-silver bimetallic nanoparticles (Au-Ag NPs) obtained from green synthesis in *Asplenium scolopendrium* L. and *Dryopteris filix-mas* (L.) Schott spores extracts. To our knowledge, this is the first report of the Au-Ag NPs phytosynthesis based on extracts obtained from fern spores. UV-Vis spectroscopy analysis of the samples revealed the maximum absorbance, characteristic of samples with bimetallic nanoparticles, which varied depending on the Au:Ag ratio. Energy-dispersive X-ray spectroscopy confirmed the presence and distribution of Au, Ag and other chemical elements. The presence of specific secondary metabolites in the extracts that helped in NPs biosynthesis stimulated growth processes. Good results

were recorded for some *Dryopteris filix-mas* samples, correlated with a significantly increased mitotic index. Cell viability decreased significantly in three of the nanoformulations. Only extracts with Au-Ag NPs showed antimicrobial effect against *Staphylococcus aureus* ATCC 25923, *Bacillus subtilis* ATCC 6633 and *Escherichia coli* ATCC 8739. The testing of the antibacterial potential of these extracts must be extended to other bacterial strains and other microorganisms, the search of new antimicrobial resources being an urgent necessity nowadays.

Keywords: spore extracts, *Asplenium scolopendrium* L., *Dryopteris filix-mas* (L.) Schott, phytosynthesis, gold-silver nanoparticles, phytotoxicity, cell viability, cytogenotoxicity, antibacterial potential.

INTRODUCTION

Green synthesis is a promising substitute for traditional synthesis methods. Among different green synthesis methods, the use of unicellular and multicellular biological entities for obtaining nanoparticles (NPs) represents one of the most promising routes (Ettadili et al. 2022). Plants produce alkaloids, flavonoids, carbohydrates, polymers, proteins, and numerous antioxidants that are efficiently used in NPs synthesis (Patel et al. 2021), because they are involved in the bioreduction of metal salts (Nasrollahzadeh et al. 2019).

According to Chatterjee et al. (2019), among Cryptogames, algae and bryophytes are the most used to obtain nanoparticles, while ferns are little investigated. Various organs of ferns can be used to obtain the extracts needed for phytosynthesis, the spores being considered in recent years (Soare and Șuțan 2018).

The antioxidant potential and medicinal value of fern species determinate their selection for the synthesis of AgNPs and AuNPs (Makarov et al. 2013). By reducing $AgNO_3$ and $HAuCl_4$ in *Adiantum philippense* extracts, AuNPs and AgNPs were obtained (Sant et al. 2013) and Kunjiappan et al. (2015) reported the synthesis of AuNPs in *Azolla microphylla* extract.

The investigation of the phytotoxicity of NPs contributes to the establishment of their toxicity profile (USEPA 2005). Seed germination, root and stem growth, and seedling biomass are the morphophysiological parameters frequently used in such studies (Drăghiceanu et al. 2019; Pathipati et al. 2018). The biochemical parameters and those related to the cytogenotoxicity of NPs (Drăghiceanu et al. 2019) are often added to the morphophysiological ones, because if the NPs or the aggregates of NPs are small, they can penetrate the cell and interact with different cellular components and induce metabolic or genetic changes (Pathipati et al. 2018).

Silver has been considered an antimicrobial agent since ancient times. The antimicrobial activity of AgNP is influenced by two important factors: the high stability of dispersion and the release of Ag ions (Harada et al. 2018). AgNPs can effectively eliminate pathogenic bacteria, and by forming alloys with other noble metals (e.g Au) the stability of these materials can be significantly improved while maintaining antibacterial activity (Qin et al. 2021).

Au-Ag NPs showed increased antimicrobial, antioxidant and anticancer activities (Godipurge et al. 2016) compared to monometallic NPs due to the interactions between the two metals that occur in fine structures determining surfaces with new characteristics (Latif-ur-Rahman et al. 2015).

The first aim of this study was to determine the ability of aqueous extracts obtained from fern spores to produce bimetallic nanoparticles (Au-Ag NPs). Secondly, we sought to characterize the extracts with NPs by UV-Vis spectroscopy (UV-Vis), scanning transmission electron microscopy coupled with energy dispersive spectroscopy (STEM-EDX), X-Ray diffraction (XRD), and test to establish their phytotoxicity, cytogenotoxicity, and antibacterial potential.

MATERIALS AND METHODS

Obtaining extracts from fern spores

The spores used for the extracts were obtained from different mature individuals plants of *Asplenium scolopendrium* L. (A) and *Dryopteris filix-mas* (L.) Schott (D) from Vâlsan Valley (Argeș, Romania). The voucher specimens were recorded in the herbarium collection of the Argeș County Museum (*Asplenium scolopendrium* – 11.331, *Dryopteris filix-mas* – 11.330) (Soare et al. 2021). The ratio between plant material (spores) and solvent (distilled water) was 1:100 (g/mL). The micrometric dimensions of the spores which form a fine powder did not require grinding of the biological material. The spores and solvent were maintained in contact at room temperature (15 °C) for 5 days then filtered. For AuNPs and AgNPs phytosynthesis, we used plant extracts (DAM, AAM), 0.1 mM $HAuCl_4$ and 1 mM $AgNO_3$, the two reagents being added in 1:1 and 1:10 proportions (AA 1:1, AA 1:10, DA 1:1, DA 1:10) (Fierăscu et al. 2017b). The experimental variants are presented in Table 1.

Table 1. Experimental variants.

Variants	Content	Dilution
Control	Distilled water	-
DAM D10	Aqueous extract of D spores	10
DAM D100		100
DA1:1 D10	Aqueous extract of D spores with bimetallic nanoparticles (Au-Ag 1:1)	10
DA1:1 D100		100
DA1:10 D10	Aqueous extract of D spores with bimetallic nanoparticles (Au-Ag 1:10)	10
DA1:10 D100		100
AAM D10	Aqueous extract of A spores	10
AAM D100		100
AA1:1 D10	Aqueous extract of A spores with bimetallic nanoparticles (Au-Ag 1:1)	10
AA1:1 D100		100
AA1:10 D10	Aqueous extract of A spores with bimetallic nanoparticles (Au-Ag 1:10)	10
AA1:10 D100		100

Note: A - *Asplenium scolopendrium* L., D - *Dryopteris filix-mas* (L.) Schott.

Physicochemical characterization of extracts

Physicochemical characterization of extracts is performed by *UV-Vis*, *STEM-EDX* (HITACHI SU8230 microscope) and XRD (Rigaku SmartLab).

The formation of the Au-Ag NPs was examined using the PerkinElmer Lambda25 UV-Vis Spectrophotometer, in the range 370-600 nm for Au-Ag NPs (Fierăscu et al. 2017b) using a 10 mm quartz cuvette with optical path.

STEM-EDX was used to confirm the presence of Au and Ag, and to investigate particles shape and size distribution. For each extract a drop was poured on STEM sample holder (Ni grid with carbon support film) and dried for 24 hours in a desiccator. For each sample EDX area scans were performed in order to obtain chemical elemental information and confirm the Au and Ag presence. Also, EDX mapping have been obtained in order to investigate Au and Ag presence and distribution. STEM images provided information about particle's shape and size distribution (Soare and Șuțan 2018).

X-Ray diffraction. The solutions containing nanoparticles dispersions were prepared for analysis by deposition on the surface of the sample holder and evaporated at room temperature for 10-15 minutes before being subjected to analysis. The XRD analysis were performed using a 9 kW Rigaku SmartLab diffractometer (Rigaku Corp., Tokyo, Japan, 45 kV and 200 mA, CuKα radiation-1.54059 Å), in scanning mode $2\theta/\theta$, between 7° and 90° (2θ). The analyzes were performed using the Rigaku Data Analysis Software PDXL 2, database provided by ICDD.

Crystallite size was determined using the Debye-Scherrer equation:

$$D_P = \frac{K \times \lambda}{\beta \times cos\theta} \quad (1)$$

where *Dp* represents the average size of the crystallites, *K* - Scherrer constant (for cubic structures, $K = 0.94$), β - the width at half-height of the diffraction maximum, θ - Bragg angle, λ - wavelength (1.54059 Å in our case).

Assessment of the phytotoxic effect by Triticum test

The seeds of *Triticum aestivum* L., Miranda variety, were provided by Agricultural Research and Development Station Pitești, Albota, Romania. The seeds were hydrated in distilled water and immersed in the test solution for 1 hour. Then, the seeds were placed in Petri dishes on filter paper and periodically watered with distilled water. The Petri dishes were kept in the dark at 20±2 °C temperature and 20±3% humidity, until the measurements were made. Ten seeds were used for each variant.

After 4 days from the beginning of the experiment the root and stem length were measured and fresh and dry weight were determinate. The dry weight was established after keeping the plant material in the oven, at 80 °C, until a constant weight was obtained (Azooz et al. 2012).

The inhibition rate of the length of root and stem seedlings was calculated using formulas (2) provided by Ma et al. (2019):

$$\text{The inhibition rate} = [(Gm-Gx)/Gm]\times 100 \quad (2)$$

where Gm - values reached for the Control determined parameters, Gx - values reached for the determined parameters for the variants with extracts.

Evaluation of cytogenotoxic effects by Allium test

After removing the cataphylls and old roots, onion bulbs (*Allium cepa* L.) of about 3.5 cm diameter were placed with the discoidal stem in distilled water and kept in the dark for 48 h at room temperature. The bulbs with new roots were transferred to the test solution for 48 hours (Table 1). The roots were stored in 70% ethanol at 2-4 °C, after they were fixed 24 hours in Farmer's solution. The squash technique was used to display in a single layer the root tips cells hydrolysed with 1N HCl and stained with 2% aceto-orcein. To evaluate the cytogenetic activity of the extracts, approximately 3000 cells/experimental variant were analysed and the mitotic

index (MI), mitosis phase indices and the frequency of chromosomal aberrations were determined (Soare and Șuțan 2018).

Evaluation of cell viability by Evans Blue test

To establish the cell viability with Evans Blue staining, we used the protocols proposed by Chen et al. (2008), Vijayaraghavareddy et al. (2017) and Adamakis et al. (2019) with minor modifications. After the experimental treatment, 10 roots from each onion bulb were randomly selected. These were immersed for 15 minutes in 2 ml of 0.25% aqueous Evans Blue solution and then rinsed with distilled water to remove excess dye. The roots were kept in distilled water overnight at room temperature. To extract the dye, the apical parts of the roots (5 mm) were excised on the next day and placed in 2 ml of 1% aqueous solution of sodium dodecyl sulfate and kept in a water bath at 50 °C for one hour. For the quantitative determination of the absorbed dye, the absorbance at 600 nm was measured using T70+ UV-Vis Spectrophotometer.

Evaluation of antimicrobial activity

The antibacterial activity of the undiluted extracts with and without Au-Ag NPs was tested against standard bacterial strains (*Escherichia coli* ATCC 8739, *Staphylococcus aureus* ATCC 25923, *Bacillus subtilis* ATCC 6633) (LTA, Italy) by Kirby-Bauer protocol on Mueller Hinton agar, according to the Clinical and Laboratory Standards Institute (CLSI) guidelines (Radji et al. 2013). For the sterilized discs (6 mm diameter) 7 µl of extract was added and after the incubation period (24 h, 37 °C), the diameter of inhibition zones around the discs was determined. The measurements were performed considering the negative (distilled water, AD) and the positive (ampicillin, ATB) control. To determine minimal inhibitory concentration (MIC), binary serial dilutions of the tested extracts were performed (according to the CLSI standard, adapted broth dilution method), in which equal amounts of microbial inoculum were inoculated (Radji et al. 2013). Equal amounts of microbial inoculum (0,5 McFarland) and broth with decreasing amounts of extracts were incubated at 37 °C for 24 h. The results were appreciated by the unaided eye, considering the control (broth tube without extract, inoculated).

The interpretation of the results was made the next day considering the following aspects: clear culture medium – without bacterial development, hazy medium – bacterial development. The MIC value was determined by calculating the arithmetic mean of the last dilution with clear culture medium and the first dilution with hazy culture medium.

Statistical analysis

Data obtained after three repetitions of *Triticum* and *Allium* tests, Evans Blue and Kirby-Bauer protocols, were statistical analysed using IBM SPSS Statistics 23. The mean and standard error (SE) were calculated, and the averages were compared with Duncan's multiple comparison test.

RESULTS AND DISCUSSION

UV-Vis Spectroscopy

UV-Vis spectroscopy is a technique used to characterize nanoparticles of noble metals and is easy to apply (Hu and Xianyu 2021). UV-Vis analysis of the samples revealed that in the case of the extracts with bimetallic nanoparticles (Figure 1), the following peaks were obtained: 533 nm (AA1:1), 521 nm (DA1:1), and 441 nm (AA1:10, DA1:10). The peak value recorded for AA1:10 and DA1:10 is closer to monometallic Ag due to the higher proportion of Ag compared to Au. Our results are confirmed by other research. The formation of bimetallic NPs is highlighted by the appearance of a single band whose peak is located between that of the AuNPs and AgNPs (Tamuly et al. 2013; Garcia et al.

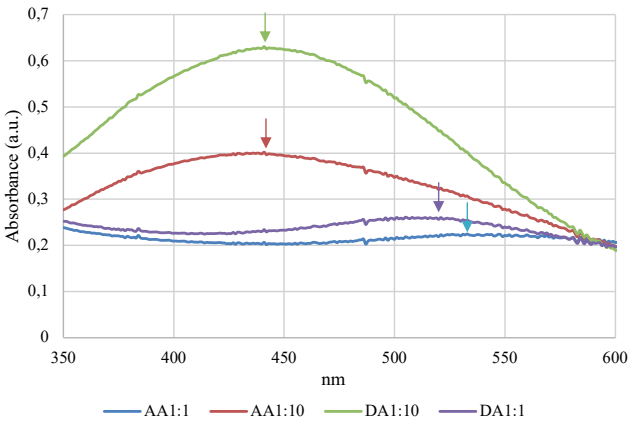

Figure 1. UV-Vis spectra of *Asplenium scolopendrium* L. and *Dryopteris filix-mas* (L.) Schott spores extracts with Au-Ag nanoparticles (AA1:1, AA1:10, DA1:1, DA1:10 sample). The arrow indicates the maximum absorbance obtained for the investigated samples.

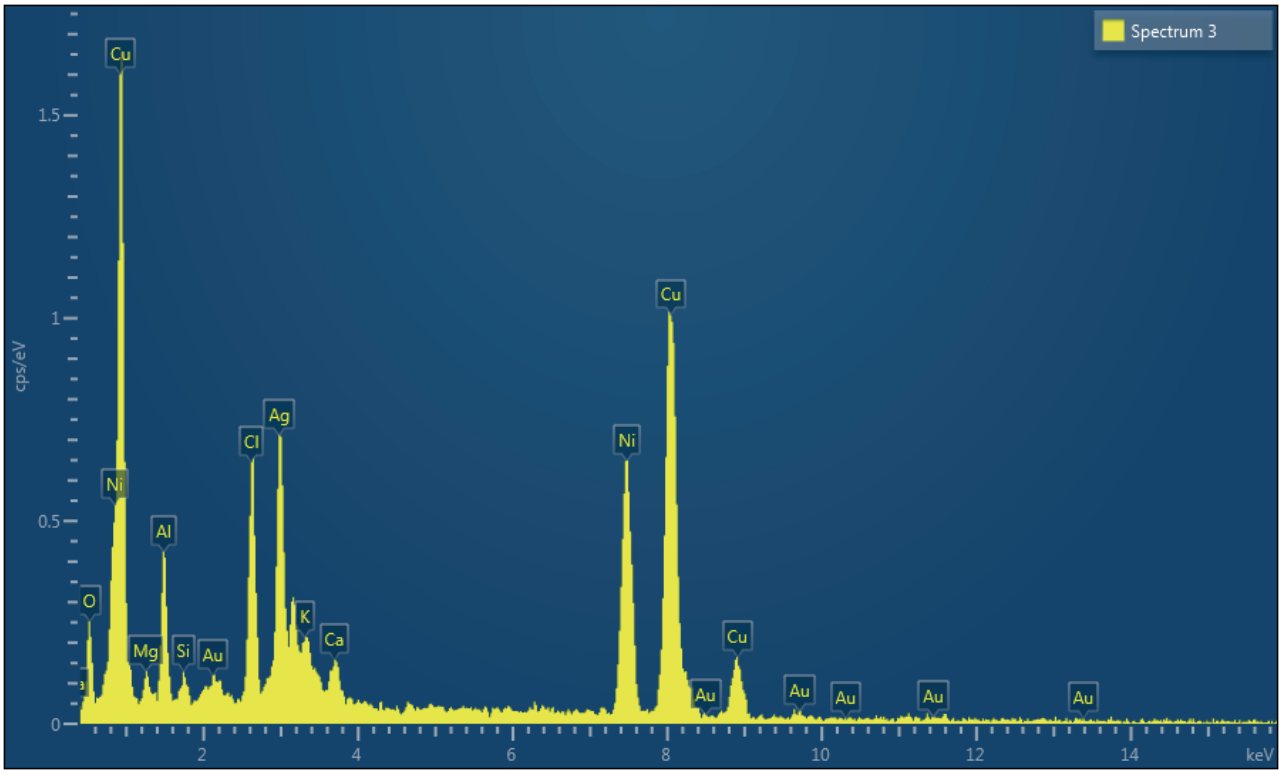

Figure 2. EDX spectra obtained for the *Asplenium scolopendrium* L. spores extract with Au-Ag nanoparticles (AA1:1 sample).

2014; Malathi et al. 2014). An example is for monometallic nanoparticles (AgNPs, AuNPs), as well as bimetallic ones (Ag-AuNPs) biosynthesized in extract obtained from the root of the medicinal plant *Plumbago zeylanica*, Salunke et al. (2014) obtained the maximum absorbance at 440 nm for Ag monometallics, at 570 nm for Au monometallics and at 540 nm for bimetallic ones. Çıplak et al. (2018) obtained a maximum absorbance at 410 nm for AgNPs and at 534 nm for AuNPs. In the case of bimetallic nanoparticles Ag67Au33, Ag50Au50 and Ag33Au67, the authors obtained different values of absorbance, depending on the Au:Ag ratio, respectively 412 nm, 519 nm and 523 nm.

In extracts with nanoparticles, the carbonyl group at 1635 cm^{-1} shows an increased intensity as a result of the capture/reduction of the metals (Drăghiceanu et al. 2021). It was also confirmed that the carbonyl group had stronger ability to bind with metal nanoparticles or act as stabilizing agents (Huleihel et al. 2002).

STEM-EDX Analysis

The investigation of the samples with EDX (Energy-dispersive X-ray spectroscopy) revealed the elemental composition (Su 2017), besides the elements added for obtaining the nanoparticles being highlighted and others (Cu, Ni, O, Al, Cl, Ca, Sn, K, and Mg), characteristic of the extracts, as it is observed from the Figures 2 and 3. The EDS mapping exposed the 2D presence and distribution of chemical elements within the investigated areas for all the samples, as can be seen for Au and Ag in *A. scolopendrium* (AA1:1) and *D. filix-mas* extracts (DA1:1) (Figure 4).

STEM analysis was used to investigate nanoparticles shape and size (Su 2017). The Au-Ag NPs obtained in the *A. scolopendrium* and *D. filix-mas* extracts had sizes between 5-39 nm for AA1:1 sample, 8-39 nm for AA1:10, 13-35 nm for DA1:1 and 15-35 nm for DA1:10 (Figure 5). Particle size between 4-94 nm and 2-78 nm, respectively, have been reported for AgNPs and AuNPs obtained by phytosynthesis assisted by various pteridophytes (Rao et al. 2021).

XRD Analysis

The crystallographic characteristics of the materials were evaluated from the diffraction pattern of the samples. Figure 6 presents the normalized spectra obtained for the four samples.

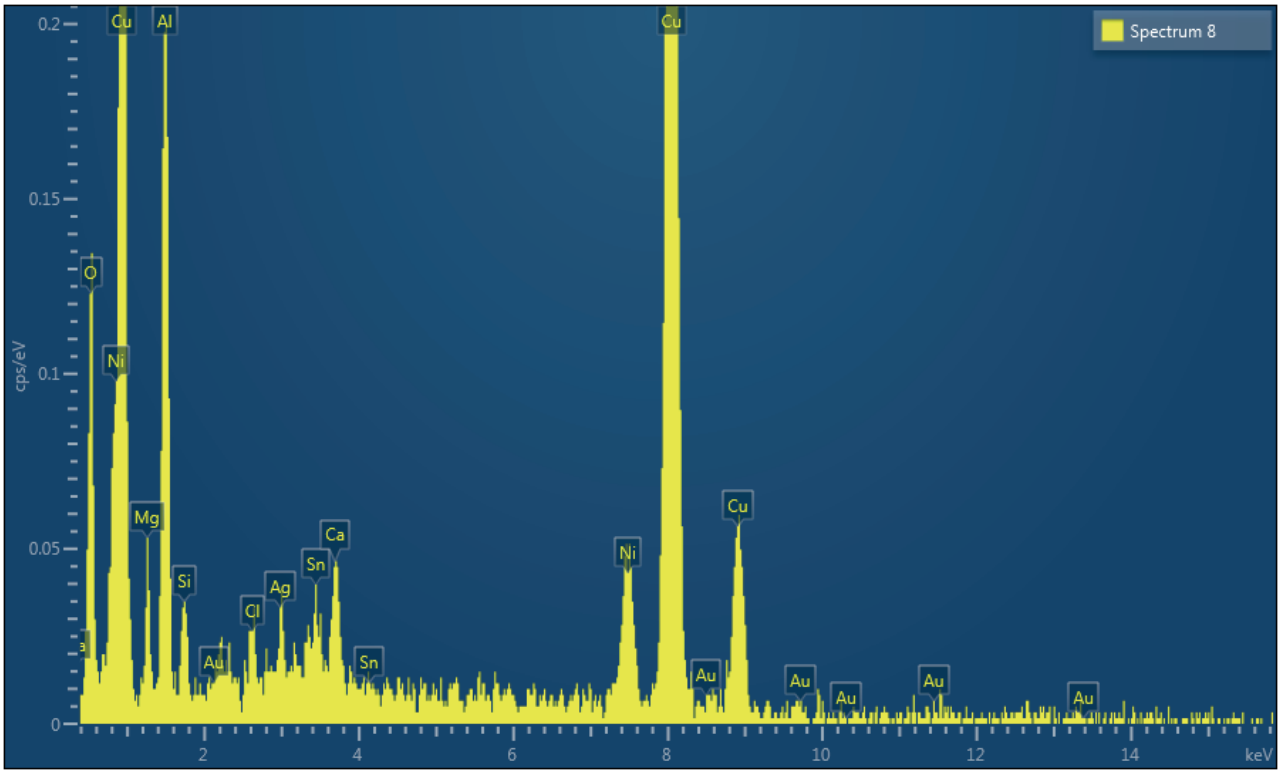

Figure 3. EDX spectra obtained for the *Dryopteris filix-mas* (L.) Schott spores extract with Au-Ag nanoparticles (DA1:1 sample).

The recorded spectra were interpreted using the dedicated software and the present phases were identified by comparison with corresponding ICDD entries. The results obtained are presented in Table 2. The identified phases were Au (ICDD card no. 00-004-0784), Ag (ICDD card no. 01-071-4613), Ag_2O (ICDD card no. 00-012-0793, marked with * on figure 6), and A_3O_4 (ICDD card no. 03-065-9750, marked with # on figure 6).

From XRD data it can be observed that all samples have a similar composition (although much well defined for sample DAA 1:10, while sample DAA 1:1 presents a much poorer defined spectra). Regarding the phases identified in the NPs solutions, it must be stated that the discrimination between Ag and Au is difficult, as the two metals exhibit similar diffraction patterns (the diffraction peaks overlapping). Also, the presence of different types of silver oxides was previously suspected to be due to oxidation of the NPs (Fierăscu et al. 2020; Șuțan et al. 2021).

Also, the identification must also consider the results obtained by other methods (especially UV-Vis and STEM-EDX). As such, samples with a lower Au:Ag ratio (AA 1:10 and DA 1:10) exhibit in the UV-Vis spectra a peak around 441 nm, which could be assigned to the presence of Ag_2O (Abouhaswa et al. 2022; Shume et al. 2020), although in our case the spectrum appears to have a small hypsocromic shift, which could be assigned to the presence of AgNPs (Bhui et al. 2009); other authors assign for the presence of Ag_2O a peak around 430 nm (Shume et al. 2020), which would imply a bathocromic shift of our spectra, which could be explained by a very small contribution of the AuNPs (suggested also by the shape of the UV-Vis spectra, slightly deformed towards higher wavelengths. The double silver oxide (Ag_3O_4) is most probably a secondary phase, formed either during reaction or during sample preparation for analysis, as other authors also noticed (Rajalakshmi et al. 2023) Samples AA and DA 1:1, presents specific UV-Vis peaks for AuNPs (above 520 nm). However, in the XRD spectra, these samples exhibit similar diffraction peaks as the other two samples. The presence of Au in the samples is also confirmed by the EDX mapping performed on the samples, as such, the most probably explanation for these two samples is that the silver / silver oxide phases are either masked by the AuNPs (in the form of core-shell structure, with the shell formed by AuNPs), which would allow the proheminent presence of AuNPs in the UV-Vis spectra, or by the oxidation of the AgNPs core during sample preparation. Our opinion, based on the analytic results, is that, for the samples

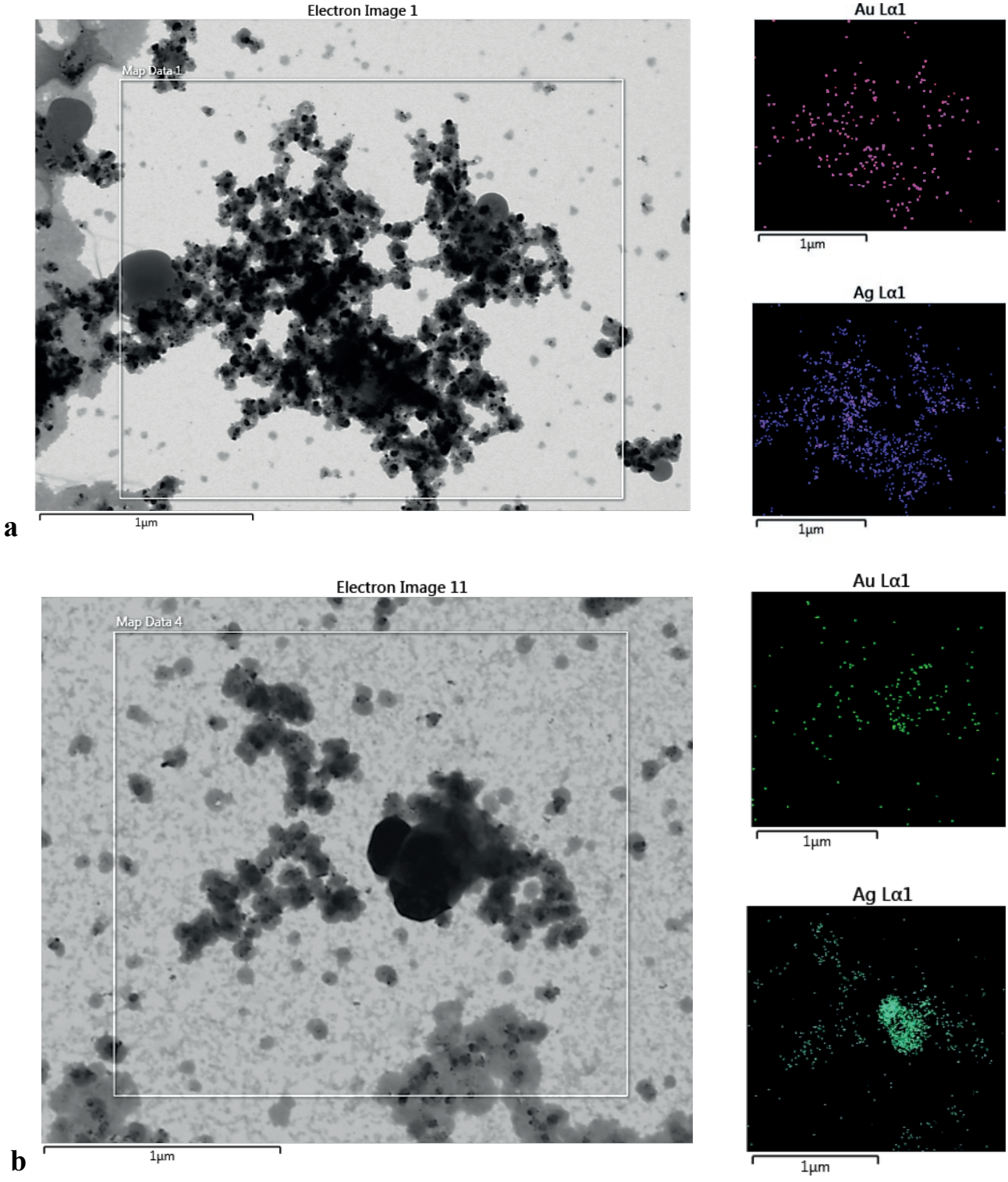

Figure 4. EDX-mapping - presence and distribution of chemical elements within the investigated areas (left): Au (right top) and Ag (right bottom) mapping in *Asplenium scolopendrium* L. spores extract with Au-Ag nanoparticles (AA1:1 sample) (**a**) and in *Dryopteris filix-mas* (L.) Schott (DA1:1 sample) (**b**).

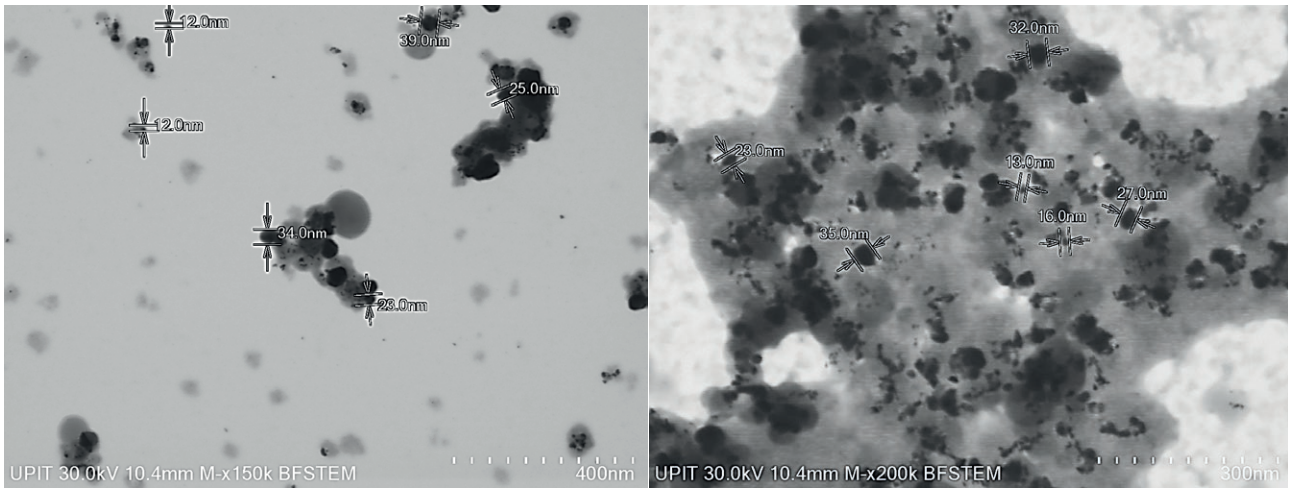

Figure 5. *Asplenium scolopendrium* L. extract with Au-Ag nanoparticles, AA1:1 sample. Au-AgNPs analysis in BFSTEM (x150k magnification) (left). *Dryopteris filix-mas* (L.) Schott extract with Au-Ag nanoparticles, DA1:1 sample. Au-AgNPs analysis in BFSTEM (x200k magnification) (right).

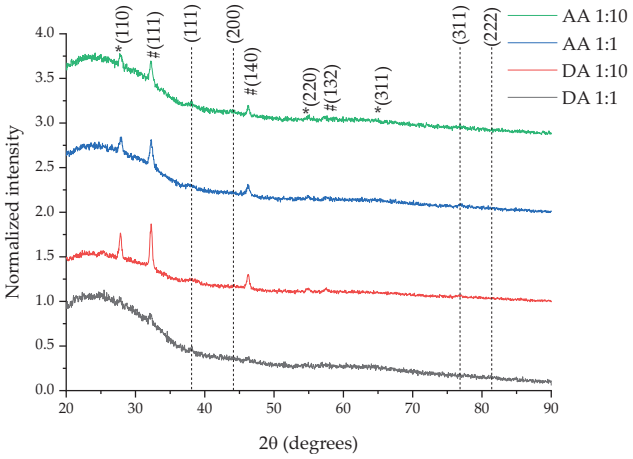

Figure 6. XRD spectra of the obtaining nanoparticles in *Asplenium scolopendrium* L. and *Dryopteris filix-mas* (L.) Schott spores extracts (blue AA 1:1, green AA 1:10, black DA1:1, red DA1:10).

with lower Au content (AA and DA 1:10) the silver/silver oxide nanoparticles with lower AuNPs content reprezent a majority phase, in the samples with a higher Au content (samples AA and DA 1:1), clusters of nanoparticles are formed, in which the AuNPs are found on the outer layer (thus contributing to the UV-Vis spectra), while the mixture of silver/silver oxide NPs found in the inner layer are re-arranged during sample preparation for XRD, which allows them to exhibit a much intense specific XRD peaks.

Assessment of the phytotoxic effects

The evaluation of phytotoxicity can be made by following some morphological, genetic, biochemical, physiological parameters, etc. *Triticum* test is frequently used for phytotoxicity studies in higher plants due to its advantages: quick results, simplified operative procedure, good reproducibility and repeatability and reduced costs (Drăghiceanu et al. 2019).

The extracts obtained, with and without NPs, stimulated the growth of the root and stem. Statistically significant differences were noticed for the root incubated in the DA1:10 D10, DA1:10 D100 samples and for the stem defined by DA1:10 D100 sample (Table 3). The insignificant growth inhibition observed in the DAM D100 sample, may be due to the decreased amount of bioactive substances, following the dilution of the sample. Fern spores contain many substances that also play a reserve role and in combating stress, such as lipids, proteins, and amino acids, such as proline, arginine, and some LEA-type proteins (late embryogenesis abundant), that promote embryo growth (López-Pozo et al. 2018). Except for the two abovementioned variants, the presence of NPs in extracts did not induce significant changes in root and stem growth. The presence of secondary metabolites in extracts cancels out the effect of nanoparticles (Zhang et al. 2021).

Wet and dry weight were not significantly influenced by the tested extracts. According to Jahn et al. (2010) the understanding of the extent of genetic variation for biomass traits in plants is limited. In a gen-

Table 2. XRD results obtained for the analyzed samples and the corresponding Miller indices.

Peak position (approx., 2q)	Sample/attribution				Crystallite size (determined using eq. (1)), nm			
	AA 1:1	AA 1:10	DA1:1	DA1:10	AA 1:1	AA 1:10	DA1:1	DA1:10
27.5	Ag_2O (110)	Ag_2O (110)	Ag_2O (110)	Ag_2O (110)	5.03	4.76	6.38	4.96
32.2	A_3O_4 (111)	A_3O_4 (111)	A_3O_4 (111)	A_3O_4 (111)	6.42	4.88	7.05	6.81
38	Au/Ag (111)	Au/Ag (111)	Au/Ag (111)	Au/Ag (111)	7.91	5.06	8.04	9.05
44.1	Au/Ag (200)	Au/Ag (111)	Au/Ag (111)	-	-	-	-	-
46.2	A_3O_4 (140)	A_3O_4 (140)	A_3O_4 (140)	A_3O_4 (140)	-	-	-	-
55	Ag_2O (220)	Ag_2O (220)	Ag_2O (220)	-	-	-	-	-
57.5	A_3O_4 (132)	A_3O_4 (132)	A_3O_4 (132)	A_3O_4 (132)	-	-	-	-
65.2	Ag_2O (311)	Ag_2O (311)	Ag_2O (311)	Ag_2O (311)	-	-	-	-
76.8	Au/Ag (311)	Au/Ag (311)	Au/Ag (311)	Au/Ag (311)	-	-	-	-
81.4	Au/Ag (222)	-	-	Au/Ag (222)	-	-	-	-

Table 3. The influence of aqueous spores extracts, with or without Au-Ag nanoparticles on *Triticum aestivum* L. parameters

Variants	Length (mm)		Phytotoxicity (%)		Weight (g)	
	Root	Stem	on root	on stem	Fresh	Dry
Control	35.93 ± 2.05^{bc}	13.93 ± 1.02^{cd}	0.00	0.00	0.82 ± 0.02^{a}	0.38 ± 0.00^{ab}
AAM D10	41.27 ± 1.76^{ab}	15.47 ± 0.81^{bcd}	-14.84	-11.00	0.87 ± 0.01^{a}	0.39 ± 0.01^{ab}
AAM D100	35.93 ± 1.65^{bc}	15.57 ± 0.69^{bcd}	0.00	-11.72	0.82 ± 0.02^{a}	0.36 ± 0.02^{ab}
DAM D10	39.40 ± 2.16^{abc}	16.77 ± 0.94^{bc}	-9.65	-20.33	0.77 ± 0.03^{a}	0.39 ± 0.02^{ab}
DAM D100	34.43 ± 2.03^{c}	13.80 ± 0.77^{d}	4.17	0.96	0.78 ± 0.04^{a}	0.35 ± 0.01^{b}
AA1:1 D10	38.20 ± 1.37^{abc}	14.90 ± 0.80^{bcd}	-6.31	-6.94	0.77 ± 0.03^{a}	0.39 ± 0.00^{ab}
AA1:1 D100	38.27 ± 1.54^{abc}	14.40 ± 0.62^{cd}	-6.49	-3.35	0.82 ± 0.06^{a}	0.38 ± 0.02^{ab}
DA1:1 D10	39.67 ± 1.92^{abc}	17.33 ± 0.59^{ab}	-10.39	-24.40	0.80 ± 0.02^{a}	0.40 ± 0.00^{a}
DA1:1 D100	38.77 ± 2.29^{abc}	14.13 ± 0.97^{cd}	-7.88	-1.44	0.84 ± 0.04^{a}	0.38 ± 0.02^{ab}
AA1:10 D10	39.70 ± 2.01^{abc}	14.50 ± 0.86^{bcd}	-10.48	-4.07	0.80 ± 0.05^{a}	0.37 ± 0.02^{ab}
AA1:10 D100	36.60 ± 1.90^{bc}	15.33 ± 0.92^{bcd}	-1.86	-10.05	0.78 ± 0.02^{a}	0.39 ± 0.02^{ab}
DA1:10 D10	44.17 ± 1.44^{a}	14.73 ± 0.76^{bcd}	-22.91	-5.74	0.75 ± 0.02^{a}	0.37 ± 0.00^{ab}
DA1:10 D100	43.63 ± 1.75^{a}	19.50 ± 1.43^{a}	-21.43	-39.95	0.80 ± 0.04^{a}	0.36 ± 0.01^{ab}

Data are shown as mean values ± SE of three replicates; a, b, c, d – interpretation of statistical significance and significant differences through Duncan's test, $p< 0.05$).

otype, wheat seed size and protein content are correlated with vigorous seedlings and higher yields biomass (Ries and Everson 1973). The seed we used in the experiment were from one wheat variety (Trivale), and the differences that appeared in dry biomass due to seed size and protein content are minimum. Hilty et al. (2021) consider that at the organ level and on short time scales, in our case wheat seeds and 4 days of growth, we can speak about growth in terms of one-dimensional elongation (roots, stems, leaves – for monocots) while growth as biomass accumulation should be used when we talk about plants and longer time scales. The biomass is the result of the photosynthesis minus photorespiration. Therefore, the biomass production can be enhanced by reducing photorespiratory losses (Peterhansel and Maurino 2010) or by increasing the photosynthesis rate and thus leaf area (Usuda 2004). Also, the leaf traits (thickness, size, shape, number etc.) are key factors in biomass production (Yang and Hwa 2008). In this study, in the short period of the experiment, the leaves didn`t appeared and the quantity of biomass produced by the stem was small. The small differences in biomass that were registered can be attributed to the depletion of the storage compounds Hilty et al. (2021), which was necessary for the root and stem growth.

Assessment of cytogenotoxic effects

Allium test is applied to determinate the effect of the plant extracts on the genetic material (Bonciu et al. 2018; Șuțan et al. 2016; Fierăscu et al. 2017a, b). The cytogenotoxic potential of various chemical agents can be assessed either by reducing or increasing of MI. In our study, statistical analysis revealed an insignificant increase in the frequency of mitotic cells in variants defined by aqueous extracts with or without Au-Ag NPs compared to the control. A significant increase of MI was determined by the aqueous extract of *D. filix-mas* spores DA1:10 D100 (Figure 7a). Similar results were reported by Șuțan et al. (2016) who found that ethanol extracts from *A. scolopendrium* leaves stimulated cell division in the root tips of *A. cepa*. In the root meristems *of A. cepa* exposed to actions of nanoparticles of iron oxide and copper, the MI increased by 10% and 5%, respectively, compared to the control, while AgNPs caused a decrease of 16% (Jasrotia et al. 2020). The stimulation of cell division and protein synthesis may be due to the electrostatic interaction of DNA and proteins caused by the penetration of AuNPs into the nucleoplasm (Balalakshmi et al. 2017). The increase in the MI in direct correlation with AuNP dose and without the appearance of chromosomal aberrations in onion meristematic root cells has also been reported by Gopinath et al. (2013). In this context, it is important to emphasize that the stimulation of cell division can have negative effects through an uncontrolled proliferation of cells (Hoshina et al. 2009).

After extract exposure of meristematic cells of *A. cepa*, prophases were observed with a higher frequency in variants with Au-Ag NPs 1:10 samples, regardless of the tested dilution. Significant differences in metaphase frequencies were observed between control and DA1:10 D100 (Figure 7b). The anaphase index does not exceed 23% in the root tip cells treated with aqueous extracts prior to or after Au-Ag NPs biosynthesis (Figure 7b) and the telophase had the lowest distribution in the observed population cells. Also, vagrants, micronucleus, binucleate cells and C-metaphase were identified in different samples. In the extracts with Au-Ag NPs DA1: 1 D10 and AA1: 10 D10, all five types of chromosomal aberrations mentioned were identified (Table 4; Figure 8). This increase in the frequency of aberrations compared to the control can be attributed to a high concentration of the phytosynthesized NPs.

Chromosomal aberrations observed by Palácio et al. (2021) in onion root meristem cells after exposure to AgNPs were delayed chromosomes, anaphase bridges, chromosome fragments and micronuclei. The authors appreciated that AgNPs disturbed the formation of the mitotic spindle, so that its partial or complete inactivation would cause the appearance of delayed chromosomes and the loss of genetic information. AgNPs can influence cell division by DNA degradation and depolymerization, their penetration into cells is facilitated by intracellular components (Kumari et al. 2009).

Rajeshwari et al. (2016) showed that AuNPs caused chromosome fragmentation, anaphase bridges, laggards, sticky chromosomes, and others abnormalities. However, it should be noted that the results found in the literature on the cytogenotoxic effect of nanoparticles depending on their concentration are contradictory. Thus, increasing the concentration of AgNPs induced a diminution in MI and the occurrence of various chromosomal aberrations, such as laggards, ring chromosomes, C-mitosis, chromosome fragmentation, nuclear membrane damage, multinuclear cells and chromatin bridges (Abdelsalam et al. 2019).

It has also been noticed that the MI and various nuclear abnormalities increased with the gradual reduction of the AgNPs diameter from 73 to 10 nm (Scherer et al. 2019). In our study, the higher frequency of chromosomal and nuclear aberrations recorded in the experimental AA1:1 D10 it may be due to the NPs with a diameter of 5-10 nm as the STEM-EDS analysis revealed.

Ahmed et al. (2018) stated that the MI modification and the induction of chromosomal aberrations could be due to the interference of the NPs with the DNA and/or the mitotic apparatus. However, we could not find similar results regarding the assessment of cytogenotoxicity of bimetallic nanoparticles on *Allium* assay.

Evaluation of cell viability by Evans blue test

The presence of Au-Ag NPs in extracts significantly influenced cell viability compared with experimental variants defined by the extracts without NPs. In the absence of NPs, the extract significant increase the cell viability compared to Control (Figure 9). At the variants DA 1:1 and AA 1:10 (diluted 10), the amount of Evans Blue absorbed by the roots of *Allium* was significantly higher than the amount obtained for the control. Zhang et al. (2019) considered that the absorption of a large amount of this dye is due to the damage of the cell membrane caused by the NPs. This situation is also confirmed by our results: for the variants with bimetallic nanoparticles dilution 100, the absorption of the Evans blue was smaller than that at dilution 10. The extracts without NPs (AAMD10, AAMD100, DAMD10, DAMD100) significantly increased the cell viability compared to Control due to the phytocompounds found in fern spores, com-

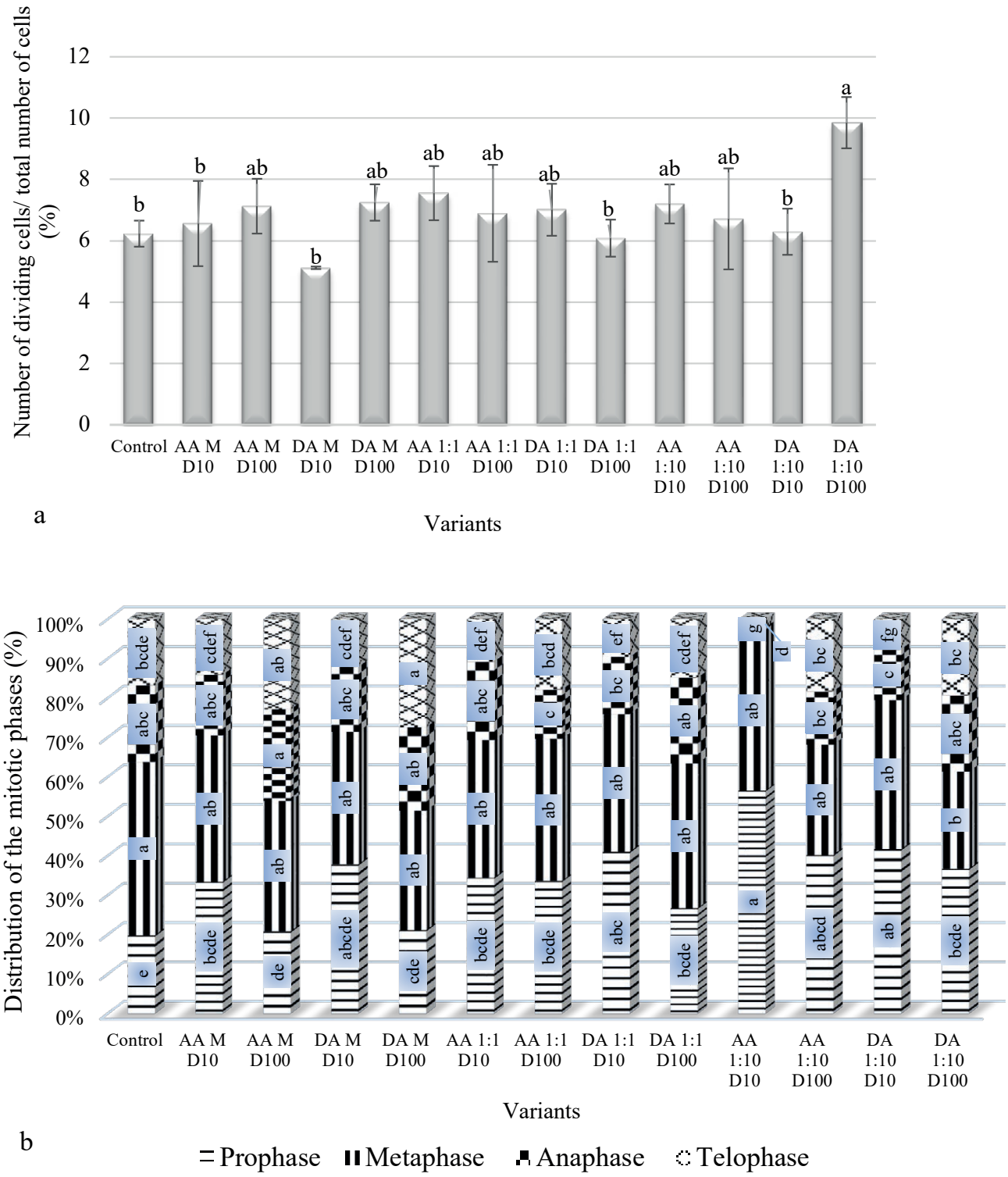

Figure 7. The influence of extracts on the mitotic index (a) and on the distribution on mitosis phase (b) in meristematic root cells of *Allium cepa* L. Data are shown as mean values ± SE of three replicates; a, b, c, d, e, f, g - interpretation of statistical significance and significant differences through Duncan's test, $p < 0.05$.

Table 4. Frequency of the main chromosomal aberrations in the meristematic root cells of *Allium cepa* L.

Variants	Chromosomal aberrations (%)				
	Anaphase bridges	Laggards	Micronucleus	Binucleate cells	C-metaphase
Control	-	1.33±1.33^{a}	-	-	-
AAM D10	19.17±3.63^{ab}	-	0.03±0.034^{a}	-	-
AAM D100	11.57±6.43^{ab}	-	-	-	-
DAM D10	11.01±2.44^{ab}	-	-	0.07±0.07^{a}	-
DAM D100	6.71±0.83^{ab}	-	-	-	-
AA1:1 D10	22.78±13.62^{a}	0.07±0.07^{a}	-	0.07±0.07^{a}	2.94±2.94^{b}
AA1:1 D100	7.50±3.82 ^{ab}	0.85±0.85^{a}	-	-	0.85±0.85^{b}
DA1:1 D10	4.86±2.50 ^{ab}	2.98±1.50^{a}	0.10±0.10^{a}	0.21±0.06^{a}	8.05±2.31^{b}
DA1:1 D100	-	2.90±2.90^{a}	-	-	4.35±2.51^{b}
AA1:10 D10	1.75±3.03^{b}	3.70±3.70^{a}	0.10±0.06^{a}	0.17±0.13^{a}	65.74±5.63^{a}
AA1:10 D100	-	-	-	-	7.69±7.69^{b}
DA1:10 D10	1.45±2.51^{b}	-	0.07±0.07^{a}	0.03±0.03^{a}	-
DA1:10 D100		-	-	0.17±0.07^{a}	-

Data are shown as mean values ± SE of three replicates; a, b, c, d, e, f, g - interpretation of statistical significance and significant differences through Duncan's test, $p< 0.05$.

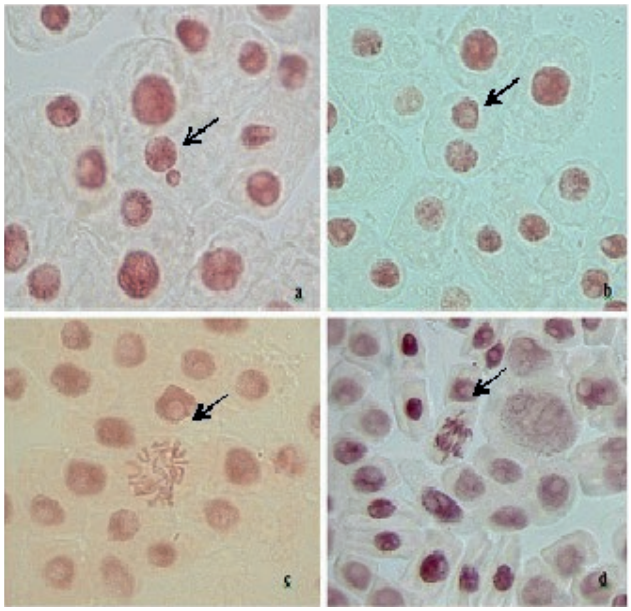

Figure 8. Chromosomal aberrations identified in the root meristem cells of *A. cepa* exposed to DA1:1 D10. (a) – micronucleus; (b) – binucleate cell; (c) – C-mitosis; (d) – vagrants.

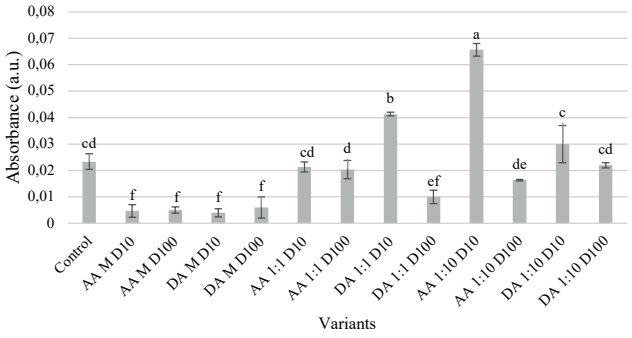

Figure 9. The influence of aqueous spores extracts, with or without Au-Ag nanoparticles, on cells viability. Data are shown as mean values ± SE of three replicates; a, b, c, d, e, f - interpretation of statistical significance and significant differences through Duncan's test, $p< 0.05$.

pounds that protect cells from stressors. The decrease of the amount of Evans blue absorbed by the roots after the treatment with various chemicals is explained by Baker and Mock (1994); they considered that the treatment can cause a large flow of electrolytes, but without necessarily causing cell death. Unlike us, after staining with Evans blue, Prajitha and Thoppil (2016) observed that aqueous extracts of *Amaranthus spinosus* L. induced cell death at the top of the *Allium* root, with the potential for membrane damage being significant. Regarding cell viability at the variants with nanoparticles diluted 100 times – we obtained similar (AA1:1, DA1:10) or greater values (DA1:1, AA1:10) compared to control. A similar situation was reported by Kannaujia et al. (2019) who studied the cell viability of the roots of two wheat varieties (HD-2967 and DBW-17) after exposure to AgNPs. After AgNPs exposure, the viability of wheat root cells assessed by Evans Blue staining was maximum in the case of wheat roots from the HD-2967 variety treated with AgNPs, while in the DBW-17 variety, the maximum viability of root cells was observed in the control and was close to that from the variant treated with AgNPs.

Antimicrobial activity of the extracts

The differences between the dimensions of inhibition zone induced by antibiotic and those induced by the aqueous extracts with bimetallic NPs are significant. The aqueous extract without NPs did not inhibit the development of bacterial strains (Figure 10b). Also, the samples DA1:10 and DA1:1 did not inhibit the growth of the *S. aureus* and *E. coli* strains. We consider that the characteristic bioactive substances of spores have a rather protective effect at the cellular level, even in the case of bacterial cells, the results being correlated with those obtained at the cell viability investigated by the Evans blue test. LEA protein, present in spores, provides protection against desiccation, osmotic, and oxidative stresses, the results being obtained using *E. coli* as an *in vivo* model to evaluate some LEA protein function (Saucedo et al. 2017).

Bimetallic nanoparticles inhibit the growth of *B. subtilis* ATCC 6633. The largest zone of inhibition of 7.17 mm was observed in the extracts with Au-Ag NPs 1:10, DA 1:10 sample (Figure 10a). A similar situation was observed for *E. coli* ATCC 8739, where the zone of inhibition was 8.83 mm in AA1:10 sample and 8 mm in DA1:10 sample (Figure 10a).

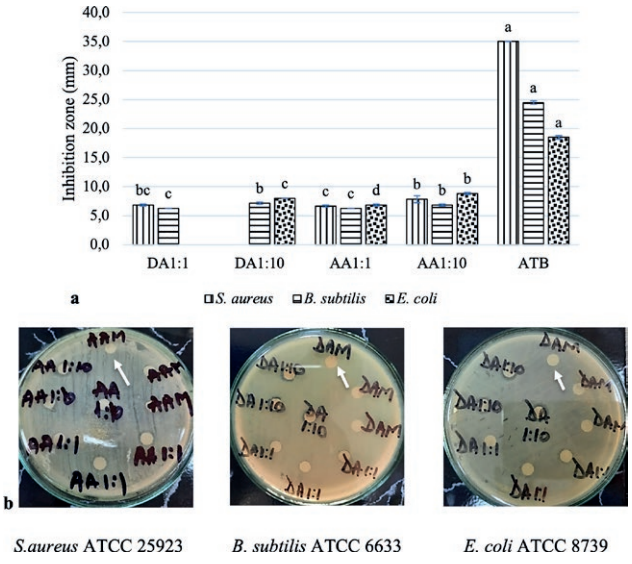

Figure 10. The antibacterial potential of the aqueous spores' extracts. Influence of extracts on *Staphylococcus aureus* ATCC 25923, *Bacillus subtilis* ATCC 6633, *Escherichia coli* ATCC 8739. The samples DA1:10 and DA1:1 did not inhibit the growth of the *S. aureus* and *E. coli* strain (**a**). Also, the aqueous extracts without nanoparticles had no antimicrobial effect, as seen (arrow) (**b**). The extract with nanoparticle may produce zone of inhibition like AA1:10 in *S. aureus*, DA1:10 in *B. subtilis*, and *E. coli* or may not produce inhibition zone in the tested strains, like DA1:1 in *E. coli*.

Table 5. Minimum inhibitory concentration (ml extract/ml medium).

Experimental variants	Bacterial strain		
	Bacillus subtilis A TCC 6633	*Escherichia coli* ATCC 8739	*Staphylococcus aureus* ATCC 25923
DA1:1	0.187	Nt	0.046
DA1:10	0.046	0.093	Nt
AA1:1	0.093	0.375	0.187
AA1:10	0.093	0.046	0.093

Note: Nt-not determined.

Aqueous extracts of spores of *A. scolopendrium* with Au-AgNPs had a higher antimicrobial efficiency in *S. aureus* ATCC 25923 than extracts of spores of *D. filix-mas* (Figure 10a). The influence of extracts on *S. aureus* ATCC 25923, *B. subtilis* ATCC 6633, *E. coli* ATCC 8739 are observed in Figure 10b.

MIC determined only for variants that had antimicrobial effect (Table 5) was between 0.046 ml extract for DA1:10 and AA1:10/ml medium in *B. subtilis* and *E. coli* and 0.187 ml extract for DA1:1 and AA1:1/ml medium in *B. subtilis* and *S. aureus* (Figure 11).

Au-Ag NPs strongly inhibited *B. subtilis* growth compared to control and monometallic nanoparticles; a similar situation was observed for *E. coli* (Reddy et al. 2012). The increase in the number of Ag ions released from bimetallic nanoparticles indicates that Au ions influence the oxidation of Ag atoms (Harada et al. 2018). Green-synthesized Ag-Au NPs exhibited promising antibacterial activity against *E. coli*, *B. subtilis*, *Klebsiella pneumoniae*, *Pseudomonas aeruginosa*, and *S. aureus* in a dose-dependent manner (Amina et al. 2020). The antibacterial potential of plant extracts with bimetallic Ag-Au NPs depends on particle size, shape, area and surface polarity, morphology, and plant specific compounds (Amina et al. 2020). Spore-specific bioactive compounds allowed the production of green bimetallic nanoparticles, which have superior properties to those obtained by chemical synthesis, being less phytotoxic, biocompatible, environmentally friendly, which might be due to the capping of biomolecule onto the surface of NPs (Panicker et al. 2020).

CONCLUSIONS

The aqueous extracts obtained from the spores of the native ferns *A. scolopendrium* and *D. filix-mas* constituted optimal media for the biosynthesis of Au-Ag

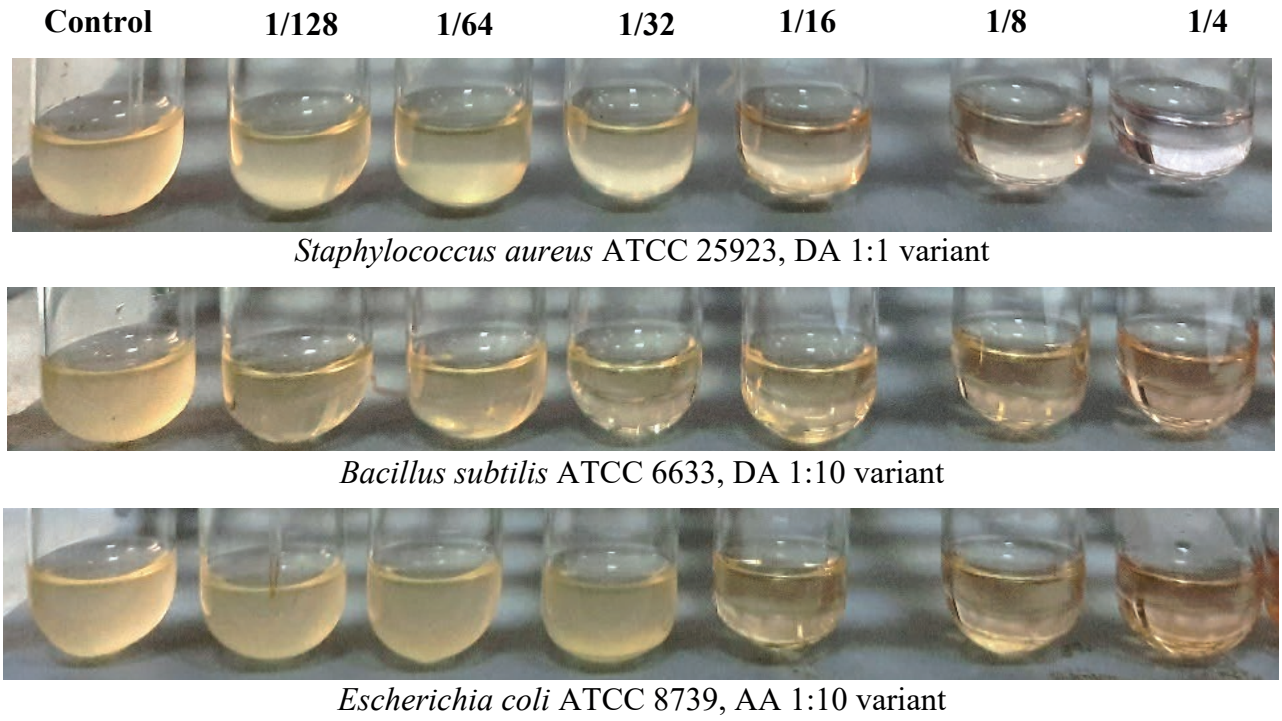

Figure 11. Aspects of MIC evaluation. Control (broth tube without extract), bacterial cultures obtained in various extract dilutions (1/128, 1/64, 1/32, 1/4).

NPs. The growth processes evaluated in the seedlings of *Triticum aestivum* were, in general, stimulated by both categories of extracts, with and without NPs, significant differences being obtained for those of *D. filix-mas*. The effect of stimulating the growth of axial organs was also confirmed by the results obtained in the *Allium* test. Extracts without NPs significantly improved cell viability, assessed by the Evans blue test, alongside the variant with NPs, DA1:1 D100. An antimicrobial effect was observed just for sample with bimetallic NPs, against all three bacterial strains: *S. aureus* ATCC 25923, *B. subtilis* ATCC 6633 and *E. coli* ATCC 8739. The sample with aqueous extract without NPs did not inhibit the development of bacterial strains. The increase in antibiotic resistance of microorganisms requires the discovery of new products with such properties, so it is useful to continue the research of less evaluated resources, such as fern spores.

ACKNOWLEDGEMENT

O.A.L. thanks the University of Pitesti for the financial support through the grant no. CIPCS-2020-08. N.A.Ş. thanks the Romanian Ministry of Education and Research, CNCS-UEFISCDI, for the financial support through the Project number PN-III-P4-ID-PCE-2020-0620, within PNCDI III. IF and RCF also acknowledge the support obtained through a grant of the Ministry of Research, Innovation and Digitization, CNCS/CCCDI-UEFISCDI, project number PN-III-P2-2.1-PED-2021-0273, grant no. 644PED/2022, within PNCDI III.

FUNDING

This research was funded by University of Pitesti through the grant no. CIPCS-2020-08, Romanian Ministry of Education and Research, CNCS-UEFISCDI, for the through the Project number PN-III-P4-ID-PCE-2020-0620, and CNCS/CCCDI-UEFISCDI through the project number PN-III-P2-2.1-PED-2021-0273, grant no. 644PED/2022.

AUTHOR CONTRIBUTIONS

Conceptualization: OAL, LCS, NAŞ, IF, RCF, DN; experimental design and laboratory work: OAL, LCS,

IF, RCF, CMD, AP, CMP, CMT, LEV, ID, DN, DȘV, GC, FA, SOH, NAȘ; funding acquisition: OAL, NAȘ, IF, RCF. Writing, review and editing: all authors.

REFERENCES

Abdelsalam NR, Fouda MMG, Abdel-Megeed A, Ajarem J, Allam AA, El-Naggar ME. 2019. Assessment of silver nanoparticles decorated starch and commercial zinc nanoparticles with respect to their genotoxicity on onion. Int J Biol Macromol. 133:1008-1018. https://doi.org/10.1016/j.ijbiomac.2019.04.134

Abouhaswa AS, Almurayshid M, Almasoud F. Sayyed MI, Mahmoud KA. 2022. Examinations the optical, mechanical, and shielding properties of Ag_2O doped B_2O_3–Bi_2O_3–SrF_2–Na_2O glasses for gamma ray shield applications. Sci Rep. 12:3548. https://doi.org/10.1038/s41598-022-07450-7

Adamakis I-D, Eleftheriou E. 2019. Structural evidence of programmed cell death induction by tungsten in root tip cells of *Pisum sativum*. Plants 8(3):62. https://doi.org/10.3390/plants8030062

Ahmed B, Shahid M, Khan MS, Musarrat J. 2018. Chromosomal aberrations, cell suppression and oxidative stress generation induced by metal oxide nanoparticles (MONPs) in onion (*Allium cepa*) bulb. Metallomics 10(9):1315-1327. https://doi.org/10.1039/c8mt00093j

Amina M, Al Musayeib NM, Alarfaj NA, El-Tohamy MF, Al-Hamoud GA. 2020. Antibacterial and immunomodulatory potentials of biosynthesized Ag, Au, Ag-Au bimetallic alloy nanoparticles using the *Asparagus racemosus* root extract. Nanomat. 10(12): 2453. https://doi.org/10.3390/nano10122453

Azooz MM, Abou-Elhamd MF, Al-Fredan MA. 2012. Biphasic effect of copper on growth, proline, lipid peroxidation and antioxidant enzyme activities of wheat (*Triticum aestivum* cv. *Hasaawi*) at early growing stage. Austal J Crop Sci. 6(4):688-694.

Baker CJ, Mock NM. 1994. An improved method for monitoring cell death in cell suspension and leaf disc assays using Evans blue. Plant Cell Tiss Organ Cult. 39:7-12.

Balalakshmi C, Gopinath K, Govindarajan M, Lokesh R, Arumugam A, Alharbi NS, Kadaikunnan S, Khaled JM, Benelli G. 2017. Green synthesis of gold nanoparticles using a cheap *Sphaeranthus indicus* extract: Impact on plant cells and the aquatic crustacean *Artemia nauplii*. J Photochem Photobiol B: Biol. 173:598-605. https://doi.org/10.1016/j.jphotobiol.2017.06.040

Bhui DP, Bar H, Sarkar P, Sahoo GP, De SP, Misra A, 2009. Synthesis and UV-Vis spectroscopic study of silver nanoparticles in aqueous SDS solution. J Mol Liquids 145(1):33-37. https://doi.org/10.1016/j.molliq.2008.11.014

Bonciu E, Firbas P, Fontanetti CS, Wusheng J, Karaismailoğlu MC, Liu D, Menicucci F, Pesnya DS, Popescu A, Romanovsky AV, Schiff S, Ślusarczyk J, de Souza CP, Srivastava A, Sutan A, Papini A. 2018. An evaluation for the standardization of the *Allium cepa* test as cytotoxicity and genotoxicity assay. Caryologia 71(3):191-209. https://doi.org/10.1080/00087114.2018.1503496

Chatterjee A, Khatua S, Acharya K, Sarkar J. 2019. A green approach for the synthesis of antimicrobial bio-surfactant silver nanoparticles by using a fern. Dig J Nanomater Biostruct. 14(2):479-490.

Chen PY, Lee KT, Chi WC, Hirt H, Chang CC, Huang H.J. 2008. Possible involvement of MAP kinase pathways in acquired metal-tolerance induced by heat in plants. Planta 228(3):499-509. https://doi.org/10.1007/s00425-008-0753-x

Çıplak Z, Gökalp C, Getiren B, Yıldız A, Yıldız N, 2018. Catalytic performance of Ag, Au and Ag-Au nanoparticles synthesized by lichen extract. Green Process Synth 7:433-440. https://doi.org/10.1515/gps-2017-0074

Drăghiceanu OA, Fierăscu I, Fierăscu RC, Bradzis R, Dobrescu CM, Soare LC. 2019. Considerations regarding the *Triticum* phytotoxicity test. Curr Trends Nat Sci. 8(15):48-55.

Drăghiceanu OA, Șuțan AN, Dobrescu CM, Bătut-Andrei ND, Soare LC, Topală CM. 2021. Characterization in terms of composition and phytotoxicity of aqueous spores extract. Curr Trends Nat Sci. 10(20):53-60. https://doi.org/10.47068/ctns.2021.v10i20.008

Ettadili FE, Aghris S, Laghrib F, Farahi A, Saqrane S, Bakasse M, Lahrich S, El Mhammedi MA. 2022. Recent advanced in the nanoparticles synthesis using plant extract: applications and future recommendations. J Mol Struct. 1248:131538. https://doi.org/10.1016/j.molstruc.2021.131538

Fierăscu I, Milen IG, Ortan A, Fierăscu RC, Avramescu SM, Ionescu D, Șuțan A, Brînzan A, Ditu LM. 2017a. Phyto-mediated metallic nanoarchitectures *via Melissa officinalis* L.: synthesis, characterization and biological properties. Sci Rep. 7:12428. https://doi.org/10.1038/s41598-017-12804-7

Fierăscu RC, Milen IG, Fierăscu I, Ungureanu C, Avramescu SM, Ortan A, Georgescu MI, Șuțan, NA, Zanfirescu A, Dinu-Pirvu CE, Velescu BS, Anuta V. 2017b. Mitodepressive, antioxidant, antifungal and

anti-inflammatory effects of wild-growing Romanian native *Arctium lappa* L. (*Asteraceae*) and *Veronica persica* Poiret (*Plantaginaceae*). Food Chem Tox. 111:44-52. https://doi.org/10.1016/j.fct.2017.11.008

Fierăscu RC, Fierăscu I, Lungulescu EM, Nicula N, Somoghi R, Dițu LM, Ungureanu C, Șuțan AN, Drăghiceanu OA, Păunescu A, Soare LC. 2020. Phytosynthesis and radiation-assisted methods for obtaining metal nanoparticles. J Mat Sci. 55:1915-1932. https://doi.org/10.1007/s10853-019-03713-3

Garcia AG, Lopes PP, Gomes JF, Pires C, Ferreira EB, Lucena RGM, Gasparotto LHS, Tremiliosi-Filho G. 2014. Eco-friendly synthesis of bimetallic AuAg nanoparticles. New J. Chem. 38(7):2865-2873. https://doi.org/10.1039/c4nj00041b

Godipurge SS, Yallappa S, Biradar NJ, Biradar JS, Dhananjaya BL, Hedge G, Jagadish K, Hedge G. 2016. A facile and green strategy for the synthesis of Au, Ag, and Au-Ag alloy nanoparticles using aerial part of *R. hypocrateriformis* extract and their biological evaluation, Enz. Microb. Technol. 95:174-184. https://doi.org/10.1016/j.enzmictec.2016.08.006

Gopinath K, Venkatesh KS, Ilangovan R, Sankaranarayanan K, Arumugam A. 2013. Green synthesis of gold nanoparticles from leaf extract of *Terminalia arjuna*, for the enhanced mitotic cell division and pollen germination activity. Ind Crops Prod. 50:737-742. https://doi.org/10.1016/j.indcrop.2013.08.060

Harada A, Ichimaru H, Kawagoe T, Tsushida M, Niidome Y, Tsutsuki H, Sawa T, Niidome T. 2018. Gold-Treated Silver Nanoparticles Have Enhanced Antimicrobial Activity. Bull Chem Soc Japan. 92:297-301. https://doi.org/10.1246/bcsj.20180232

Hilty J, Muller B, Pantin F, Leuzinger S. 2021. Plant growth: the What, the How, and the Why. New Phytol. 232(1):25-41. https://doi.org/10.1111/nph.17610

Hoshina M, Marin-Morales M.A. 2009. Micronucleus and chromosome aberrations induced in onion (*Allium cepa*) by a petroleum refinery effluent and by river water that receives this effluent. Ecotoxicol Environ Saf. 72:2090-209. https://doi.org/10.1016/j.ecoenv.2009.07.002

Hu J, Xianyu Y. 2021. When nano meets plants: A review on the interplay between nanoparticles and plants. Nano Today 38:101143. https://doi.org/10.1016/j.nantod.2021.101143

Huleihel M, Salman A, Erukhimovich V, Ramesh J, Hammody Z, Mordechai S. 2002. Novel optical method for study of viral carcinogenesis *in vitro*. J Biochem Biophys Meth. 50:111-121. https://doi.org/10.1016/s0165-022x(01)00177-4

Jahn CE, Mckay JK, Mauleon R, Stephens J, McNally KL, Bush DR, Leung H, Leach JE. 2010. Genetic Variation in Biomass Traits among 20 Diverse Rice Varieties. Plant Physiol. 155(1):157-168. https://doi.org/10.1104/pp.110.165654

Jasrotia T, Chaudhary S, Kaushik A, Kumar R, Chaudhary GR. 2020. Green chemistry-assisted synthesis of biocompatible Ag, Cu, and Fe_2O_3 nanoparticles. Mat Today Chem. 15:100214. https://doi.org/10.1016/j.mtchem.2019.100214.2

Kannaujia R, Srivastava CM, Prasad V, Singh BN, Pandey V. 2019. *Phyllanthus emblica* fruit extract stabilized biogenic silver nanoparticles as a growth promoter of wheat varieties by reducing ROS toxicity. Plant Physiol Biochem. 142:460-471. https://doi.org/10.1016/j.plaphy.2019.08.008

Kumari M, Mukherjee A, Chandrasekaran N. 2009. Genotoxicity of silver nanoparticles in *Allium cepa*. Sci Total Environ. 407:5243-5246. https://doi.org/10.1016/j.scitotenv.2009.06.024

Kunjiappan S, Bhattacharjee C, Chowdhury R. 2015. Hepatoprotective and antioxidant effects of *Azolla microphylla* based gold nanoparticles against acetaminophen induced toxicity in a fresh water common carp fish (*Cyprinus carpio* L.). Nanomed J. 2(2):88-110. https://doi.org/10.7508/nmj.2015.02.002

Latif-ur-Rahman, Shah A, Khan SB, Asiri AM, Hussain H, Han C, Qureshi R, Ashiq MN, Zia MA, Ishaq M, Kraatz HB. 2015. Synthesis, characterization, and application of Au-Ag alloy nanoparticles for the sensing of an environmental toxin, pyrene. J Appl Electrochem. 45(5):463-472. https://doi.org/10.1007/s10800-015-0807-2

López-Pozo M, Fernández-Marín B, García-Plazaola JY, Ballesteros D. 2018. Desiccation Tolerance in Ferns: From the Unicellular Spore to the Multi-tissular Sporophyte. In Fernández H. editor. Current Advances in Fern Research. Springer, Cham; p. 401-426, https://doi.org/10.1007/978-3-319-75103-0_19

Makarov VV, Love AJ, Sinitsyna OV, Makarova SS, Yaminsky IV, Taliansky ME, Kalinina NO. 2014. "Green" nanotechnologies: synthesis of metal nanoparticles using plants. Acta Nat. 6(1):35-44.

Malathi S, Ezhilarasu T, Abiraman T, Balasubramanian S. 2014. One pot green synthesis of Ag, Au and Au-Ag alloy nanoparticles using isonicotinic acid hydrazide and starch. Carb Pol. 111:734-743. https://doi.org/10.1016/j.carbpol.2014.04.105

Nasrollahzadeh M, Sajjadi M, Sajadi SM, Issaabadi Z. 2019. Green Nanotechnology. In An Introduction to Green Nanotechnology, Nasrollahzadeh, M, Sajadi, S.M., Sajjadi, M., Issaabadi, Z., Atarod, M., Editors, Elsevier, Interface Science and Technology, pp 145-198. https://doi.org/10.1016/b978-0-12-813586-0.00005-5

Palácio SM, de Almeida JCB, de Campos ÉA, Veit MT, Ferreira LK, Deon MTM. 2021. Silver nanoparticles effect on *Artemia salina* and *Allium cepa* organisms: influence of test dilution solutions on toxicity and particles aggregation. Ecotoxicol. 30(5):836-850. https://doi.org/10.1007/s10646-021-02393-7

Panicker S, Ahmady IM, Han C, Chehimi M, Mohamed AA. 2020. On demand release of ionic silver from gold-silver alloy nanoparticles: fundamental antibacterial mechanisms study. Mat Today Chem. 16:100237. https://doi.org/10.1016/j.mtchem.2019.100237

Patel AK, Gupta D, Singh A, Mishra VK, Sharma NK. 2021. Green - synthesized nanoparticles for treatment of wastewater: an environmentally sustainable pollution remediation technology. In Sustainable Environmental Clean-up, Green Remedation; Mishra VK, Kumar A, Eds., Elsevier, pp. 29-70. https://doi.org/10.1016/B978-0-12-823828-8.00002-5.

Pathipati UR, Kanuparthi PL. 2018. Biological and Phytotoxic Impacts of a Nanomaterial. In *Phytotoxicity of Nanoparticles*; Faisal, M., Saquib Q., Alatar, A.A., Al-Khedhairy, A.A., Eds., Springer Cham., pp. 229-240. https://doi.org/10.1007/978-3-319-76708-6_9

Peterhansel C, Maurino VG. 2010. Photorespiration Redesigned. Plant Physiol, 155(1):49-55. https://doi.org/10.1104/pp.110.165019

Prajitha V, Thoppil JE. 2016. Cytotoxic and apoptotic activities of extract of *Amaranthus spinosus* L. in *Allium cepa* and human erythrocytes. Cytotechnol. 69(1):123-133. https://doi.org/10.1007/s10616-016-0044-5

Qin Z, Zheng Y, Wang Y, Du T, Li C, Wang X, Jiang H. 2021. Versatile roles of silver in Ag-based nanoalloys for antibacterial applications, Coord Chem Rev. 449, 214218. https://doi.org/10.1016/j.ccr.2021.214218

Radji M, Agustama RA, Elya B, Tjampakasari CR. 2013. Antimicrobial activity of green tea extract against isolates of methicillin-resistant *Staphylococcus aureus* and multi-drug resistant *Pseudomonas aeruginosa*. Asian Pac J Trop Biomed. 3(8):663-667. https://doi.org/10.1016/S2221-1691(13)60133-1

Rajalakshmi TU, Sheeba H, Doss A, Veerabahu R, Sivagnanam A, Alfarraj S, Alharbi SA, Subbiah J, Mariselvam R. 2023. Synthesis of silver nanoparticles from natural derived embelin compound and their uses in mercury degradation under solar light. Mat Res Express. 10(5):055502. https://doi.org/10.1088/2053-1591/acd2ad

Rajeshwari A, Roy B, Chandrasekaran N, Mukherjee A. 2016. Cytogenetic evaluation of gold nanorods using *Allium cepa* test. Plant Physiol Biochem. 109:209-219. https://doi.org/10.1016/j.plaphy.2016.10.003

Rao KJ, Korumilli T, Jakkala S, Singh K, Vidya K. 2021. Optimization of the one-step green synthesis of silver and gold nanoparticles using aqueous *Athyrium filix femina* extract using the Taguchi method. BioNanoSci. 11:915-922. https://doi.org/10.1007/s12668-021-00909-3

Reddy RP, Varaprasad K, Narayana Reddy, N., Mohana Raju, K., Reddy, N.S. 2012. Fabrication of Au and Ag bi-metallic nanocomposite for antimicrobial applications. J Appl Polymer Sci. 125(2):1357-1362. https://doi.org/10.1002/app.35192

Ma C, He M, Zhong Q, Ouyang W, Lin C, Liu X. 2019. Uptake, translocation and phytotoxicity of antimonite in wheat (*Triticum aestivum*), The Sci Total Environ. 669:421-430. https://doi.org/10.1016/j.scitotenv.2019.03.145

Ries SK, Everson EH. 1973. Protein content and seed size relationships with seedling vigor of wheat cultivars. Agron J. 65:884-886.

Salunke GR, Ghosh S, Kumar RJS, Khade S, Vashisth P, Kale T, Chopade S, Pruthi V, Kundu G, Bellare JR, Chopade BA, 2014. Rapid efficient synthesis and characterization of silver, gold, and bimetallic nanoparticles from the medicinal plant *Plumbago zeylanica* and their application in biofilm control. Int J Nanomed. 9:2635-2653. https://doi.org/10.2147/ijn.s59834

Sant DG, Gujarathi TR, Harne SR, Ghosh S, Kitture R, Kale S, Chopade BA, Pardesi KR. 2013. *Adiantum philippense* L. frond assisted rapid green synthesis of gold and silver nanoparticles. J Nanopart. 182320. https://doi.org/10.1155/2013/182320

Saucedo AL, Hernández-Domínguez EE, de Luna-Valdez LA, Guevara-García AA, Escobedo-Moratilla A, Bojorquéz-Velázquez E, del Río-Portilla F, Fernández-Velasco DA, Barba de la Rosa AP. 2017. Insights on Structure and Function of a Late Embryogenesis Abundant Protein from Amaranthus cruentus: An Intrinsically Disordered Protein Involved in Protection against Desiccation, Oxidant Conditions, and Osmotic Stress. Front Plant Sci. 8:497. https://doi.org/10.3389/fpls.2017.00497

Scherer MD, Sposito JCV, Falco WF, Grisolia AB, Andrade LHC, Lima SM, Machado G, Nascimento VA, Gonçalves DA, Wender H, Oliveira SL, Caires ARL. 2019. Cytotoxic and genotoxic effects of silver nanoparticles on meristematic cells of *Allium cepa* roots: A close analysis of particle size dependence. Sci Total Environ. 660:459-467. https://doi.org/10.1016/j.scitotenv.2018.12.444

Shume WM, Murthy HCA, Zereffa EA. 2020. A Review on Synthesis and Characterization of Ag_2O Nano-

particles for Photocatalytic Applications J Chem. 5039479. https://doi.org/10.1155/2020/5039479

Soare LC, Şuţan AN. 2018. Current trends in pteridophyte extracts: from plant to nanoparticles. In *Current Advances in Fern Research*, Fernandez H., Eds., Springer, pp. 329-357. https://doi.org/10.1007/978-3-319-75103-0_16

Soare LC, Păunescu A, Dobrescu CM, Neblea MA, Dorobăţ LM. 2021. Ferns – a valuable plant resource in modern research. In *Development of plant extracts and innovative phytosynthesized nanostructures mixtures with phytotherapeutic applications, in order to reduce biocenotic stress in horticultural crops,* Fierăscu RC, Fierăscu I, Soare LC, Eds., Ruse Press, pp. 27-44.

Su D. 2017. Advanced electron microscopy characterization of nanomaterials for catalysis. *Green Energy Environ.* 2(2):70-83. https://doi.org/10.1016/j.gee.2017.02.001

Şuţan NA, Fierăscu I, Fierăscu RC, Manolescu DS, Soare LC. 2016. Comparative analytical characterization and *in vitro* cytogenotoxic activity evaluation of *Asplenium scolopendrium* L. leaves and rhizome extracts prior to and after Ag nanoparticles phytosynthesis. Ind Crops Prod. 83:379-386. https://doi.org/10.1016/j.indcrop.2016.01.011

Şuţan NA, Fierăscu I, Şuţan C, Soare LC, Neblea AM, Somoghi R, Fierăscu RC. 2021. In vitro mitodepressive activity of phytofabricated silver oxide nanoparticles (Ag_2O-NPs) by leaves extract of *Helleborus odorus* Waldst. & Kit. ex Willd, Mat Lett. 286:129194. https://doi.org/10.1016/j.matlet.2020.129194

Tamuly C, Hazarika M, Borah SC, Das MR, Boruah MP. 2013. *In situ* biosynthesis of Ag, Au and bimetallic nanoparticles using *Piper pedicellatum* C.DC: Green chemistry approach. Coll Surf B: Biointerf. 102:627-634. https://doi.org/10.1016/j.colsurfb.2012.09.007

USEPA, 2005. Nanotechnology white paper external review draft. https://www.epa.gov/osa/pdfs/EPA_nanotechnology_white_paper_external_review_draft_12-02-2005

Usuda H. 2004. Evaluation of the effect of photosynthesis on biomass production with simultaneous analysis of growth and continuous monitoring of CO_2 exchange in the whole plants of radish, cv Kosena under ambient and elevated CO_2. Plant Prod Sci. 7(4):386-396. https://doi.org/10.1626/pps.7.386

Vijayaraghavareddy P, Adhinarayanreddy V, Ramu SV, Sreeman S, Udayakumar M. 2017. Quantification of membrane damage/cell death using Evan's blue staining technique. Bioprot. 7(16): e2519. https://doi.org/10.21769/BioProtoc.2519

Yang XC, Hwa CM. 2008. Genetic modification of plant architecture and variety improvement in rice. Heredity 101:396-404

Zhang H, Chena S, Jia X, Huang Y, Ji R, Zhao L. 2021. Comparation of the phytotoxicity between chemically and green synthesized silver nanoparticles. Sci Total Environ. 752:142264. https://doi.org/10.1016/j.scitotenv.2020.142264

Zhang WY, Wang Q, Li M, Dang F, Zhou DM. 2019. Nonselective uptake of silver and gold nanoparticles by wheat. Nanotoxicol. 13(8):1073-1086. https://doi.org/10.1080/17435390.2019.1640909